
LEARNING SMOOTH AND FAIR REPRESENTATIONS

A PREPRINT

Xavier Gitiaux
Department of Computer Science
George Mason University
Fairfax, VA 22030
xgitiaux@gmu.edu

Huzefa Rangwala
Department of Computer Science
George Mason University
Fairfax, VA 22030
rangwala@cs.gmu.edu

June 17, 2020

ABSTRACT

Organizations that own data face increasing legal liability for its discriminatory use against protected demographic groups, extending to contractual transactions involving third parties access and use of the data. This is problematic, since the original data owner cannot ex-ante anticipate all its future uses by downstream users. This paper explores the upstream ability to preemptively remove the correlations between features and sensitive attributes by mapping features to a fair representation space. Our main result shows that the fairness measured by the demographic parity of the representation distribution can be certified from a finite sample if and only if the chi-squared mutual information between features and representations is finite. Empirically, we find that smoothing the representation distribution provides generalization guarantees of fairness certificates, which improves upon existing fair representation learning approaches. Moreover, we do not observe that smoothing the representation distribution degrades the accuracy of downstream tasks compared to state-of-the-art methods in fair representation learning.

Keywords Machine Learning · Fairness · Representations · Neural Network

1 Introduction

Organizations dealing with data could function as a **data controller** that determines the purposes and means of processing the data and/or as a **data processor** that processes the data on behalf of the controller. This distinction has legal ramifications, including challenges related to the discriminatory use of data. For example, the European Union’s General Data Protection Regulation (GDPR, Article 4) holds the data controller accountable for the collection, use and disposal of the data, including the responsibility of discriminatory on the basis of sensitive attributes (e.g. racial or ethnic origin, sexual orientation, (GDPR, Recital 71)).

However, ex-ante a data controller cannot anticipate what machine learning algorithms a data processor may use to perform its task. Therefore, any contract between a data controller and a data processor is likely to be incomplete and lacks sufficient instructions to guarantee the fairness of any data processor’s application. This is problematic since a growing body of evidence has raised concerns about the fairness of machine learning outcomes across a wide range of applications, including judicial decisions ([1]), face recognition ([2]), degree completion ([3]) or medical treatment ([4]).

One promising avenue is for data controllers to limit the data access to fair representations of data instead of the data itself (e.g [5], [6], [7], [4] or [8]). Fair representation learning seeks to map the original data distribution into a distribution that retains the information contained in the original data, while being statistically independent of sensitive attributes (see Figure 1). However, current fair representation learning approaches provide fairness guarantees only against *some* pre-specified data processors ([9]). *This paper explores conditions on the encoder to generate representation distributions with fairness guarantees that hold for any data processor.*

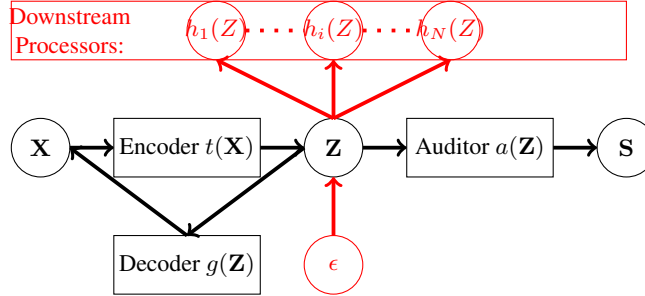


Figure 1: Fair representation learning. Variables are: features \mathbf{X} ; sensitive attribute \mathbf{S} ; representation \mathbf{Z} . The standard fair representation protocol includes an encoder t that maps X to its representation Z ; a decoder g that reconstructs X from Z ; and, an auditor a that measures the statistical dependence between Z and S ; many downstream data processors h_1, \dots, h_N that uses the representation Z . The contribution of this paper is to add an additive Gaussian white noise (AWGN) channel – i.e, a convolution step that adds a Gaussian noise ϵ to $t(\mathbf{X})$ – so that fairness guarantees can be established for all data processors h using Z .

Data controllers would like to produce fairness certificates that measure the potential unfairness of all downstream data processors who access samples from the representation distribution. The question is whether fairness certificates can be approximated by empirical certificates estimated from a finite sample. Our main result shows that for this approximation property of empirical fairness certificates to hold, it is necessary for a measure of information – the χ^2 mutual information – between feature and representation to be finite. Moreover, we prove that a finite χ^2 mutual information between feature and representation is a sufficient condition on representation mappings to guarantee a good approximate rate ($O(n^{-1/2})$) of empirical certificates.

In practice, it is challenging to establish that the χ^2 mutual information is finite without knowing the distribution over \mathcal{X} . However, we show that an additive Gaussian white noise (AWGN) channel placed after any representation mapping (see Figure 1) will bound the χ^2 mutual information once the representations have passed through the channel. The channel smoothes the representation distribution by transforming it into a mixture of Gaussian distributions that can be estimated by Monte Carlo integration ([10]). Therefore, a plug-in fairness auditor that relies on estimating the class conditional density functions over the representation space achieves a convergence rate of $O(n^{-1/2})$. Moreover, the AWGN channel offers the possibility to learn high dimensional representations without the need to resort to adversarial auditors that learn to predict the sensitive attribute from samples of the representation distribution (e.g. [5] or [7]). Instead, we approximate the empirical certificate with a differentiable loss that is computed by Monte Carlo integration.

We empirically find on various synthetic and fair learning benchmark datasets that an AWGN channel in fair representation learning is sufficient for empirical certificates to upper bound the demographic parity of multiple downstream users that attempts to predict sensitive attributes from samples of the representation distribution. An AWGN channel improves upon existing approaches in adversarial fair representation learning whose fairness guarantees do not extend beyond a set of specific downstream users. Moreover, we did not find strong evidence that obtaining good approximation rates for empirical certificates comes at the cost of significantly degrading the accuracy-fairness trade-off of downstream predictive tasks.

Related work. A growing literature explores the potential adverse implications that machine learning algorithms might have on protected demographic groups (e.g individuals self-identified as Female or African-American) ([9] for a review). Many contributions seek to define fairness criteria either at the group or individual level ([11]) and then, impose a fairness penalty into their classification algorithm (e.g. [12], [13], [14]) or audit for a specific criteria (e.g [15], [16]). In this paper, we side-step the important discussion on what fairness criteria to choose from ([17]), but investigate whether a data can be transformed so that any future use will meet a pre-specified criteria. Our results focus on demographic parity ([11]), but can be readily extended to many other group level criteria, including equalized odds and equal opportunity ([18]).

Existing pre-processing methods to mitigate unfair data use include sampling and reweighting (e.g. [19], [20]), optimization procedures to learn a data transformation that both preserve utility and limit discrimination (e.g. [21]), and representation learning (e.g. [8]). Representation learning seeks to encode the data while removing correlations between features and sensitive attributes. Recent developments in adversarial learning for generative modeling (see [22] for a survey) or domain adaptation (e.g. [23]) have spurred an interest in training a data encoder to generate a representation of the data and fool a neural network that attempts to predict sensitive attributes from samples of the

representation distribution (e.g. [7], [5], [24] or [25]). An alternative approach is to disentangle sensitive attributes from features by passing the data through an information bottleneck ([26] or [6]).

Our contribution to the fair adversarial learning literature is to explore conditions so that the learned representation offers fairness guarantees against adversaries that do not necessarily belong to the same class as the adversary used during the training of the encoder. [5] and [27] explore empirically whether representations that achieve demographic parity for a specific downstream task generalize to new tasks in terms of accuracy and fairness. We extend their work by showing theoretically and empirically that introducing an AWGN channel in fair representation learning offers generalization guarantees to all future tasks.

Similar to our approach, the differential privacy literature relies on noise injection to guarantee that two neighboring datasets are indistinguishable ([28]). However, there is an important difference between these approaches. In the context of differential privacy, indistinguishability is only obtained by adding Gaussian/Laplacian noise. In our fairness context, for a finite sample, statistical hiding comes from learning representations subject to a demographic parity constraint; the injection of Gaussian noise is only a means to generalize the statistical hiding property to the infinite sample regime. Of interest is whether this two-step approach has merits in a privacy setting.

2 Certifying Fair Representations

2.1 Background

Consider a data controller who wants to release samples from a distribution μ over $\mathcal{X} \times \mathcal{S}$ with features in $\mathcal{X} \subset [0, 1]^D$ and sensitive attributes in \mathcal{S} . Although our setup can be extended to richer spaces of sensitive attributes, we focus here on binary sensitive attributes and assume that $\mathcal{S} = \{0, 1\}$.

A transformation t that maps the features space \mathcal{X} into a representations space $\mathcal{Z} \subset \mathbb{R}^d$ induces a distribution μ_t over $\mathcal{Z} \times \{0, 1\}$: $\mu_t(A) = \mu(\{x \in \mathcal{X} | t(x) \in A\})$ for any $A \subset \mathcal{Z}$.

The data controller’s objective is to obtain a representation mapping t that minimizes the statistical dependence between representation Z and sensitive attribute S . Therefore, for any test $f : \mathcal{Z} \rightarrow \{0, 1\}$ that decides whether the class conditional distributions $\mu_t^0 = P(Z|S = 0)$ and $\mu_t^1 = P(Z|S = 1)$ are identical, the data controller would like to minimize the discrepancy

$$\Delta(f, t) \triangleq |E_{z \sim \mu_t^1}[f(z)] - E_{z \sim \mu_t^0}[f(z)]|, \quad (1)$$

where we make the dependence of Δ on representation mapping t explicit. In the context of fair machine learning, the test function f is either an auditor used by the data controller to estimate the statistical dependence between Z and S (function a in Figure 1); or, a classifier used by a data processor (function h in Figure 1) and $\Delta(f, t)$ then measures the demographic parity of f (see [18]):

Definition 2.1. Demographic parity Consider a representation distribution μ_t induced by a representation mapping $t : \mathcal{X} \rightarrow \mathcal{Z}$. A classifier $f : \mathcal{Z} \rightarrow \{0, 1\}$ used by a data processor satisfies δ -Demographic Parity on μ_t if and only if $\Delta(f, t) \leq \delta$.

Since the data controller does not know ex-ante which classifier data processors will use, she has to construct a mapping t such that all classifiers $f : \mathcal{Z} \rightarrow \{0, 1\}$ satisfy δ -demographic parity on μ_t for some pre-specified $\delta > 0$. A demographic parity certificate is therefore an upper bound on the demographic disparity of any classifiers that access samples from the representation distribution μ_t .

Definition 2.2. Demographic Parity Certificate Let $\delta \geq 0$. A representation space (\mathcal{Z}, μ_t) can be certified with δ -demographic parity if and only if

$$\Delta^*(t) \triangleq \sup_{f: \mathcal{Z} \rightarrow \{0,1\}} \Delta(f, t) \leq \delta. \quad (2)$$

To construct a representation mapping certified with $\Delta^*(t)$ -demographic parity, the data controller needs to evaluate the supremum over all test functions/auditors f_n that are constructed on the basis of a finite sample $\mathcal{D}_n = \{(x_i, s_i)\}_{i=1}^n$. Let \mathcal{F}_n denote the set of all auditors $f_n : \mathcal{Z} \times (\mathcal{Z} \times \{0, 1\})^n \rightarrow \{0, 1\}$ constructed from a sample of size n .

Definition 2.3. Empirical Demographic Parity Certificate Let $n \geq 1$ and $\delta \geq 0$. A representation space (\mathcal{Z}, μ_t) is certified with an empirical δ -demographic parity certificate if and only if

$$\Delta_n(t) \triangleq \sup_{f_n \in \mathcal{F}_n} \Delta(f_n, t) \leq \delta. \quad (3)$$

This paper investigates how to choose a representation mapping $t : \mathcal{X} \rightarrow \mathcal{Z}$ so that empirical certificates are good approximations of the true demographic parity certificate, i.e. $\Delta_n(t)$ approximates well $\Delta^*(t)$. Approximation

properties of empirical certificates are important for a data controller to anticipate the demographic parity of a downstream processor who uses fresh samples obtained after t has been constructed.

Since the data controller cannot constrain the data distribution over $\mathcal{X} \times \{0, 1\}$, we are looking for distribution-free approximation rates. In general, distribution-free rates do not exist ([29], ch. 7). But, in our setting, the data controller has some control over the representation distribution via t . In fact, the approximation $\Delta^*(t) - \Delta_n(t)$ depends on how much information in X is encoded by t in Z . If t randomly maps \mathcal{X} to \mathcal{Z} , the data controller can certify μ_t with 0-demographic parity, but μ_t is useless to downstream data processors. The data controller trades-off representation demographic parity with information by learning a representation mapping $t : \mathcal{X} \rightarrow \mathcal{Z}$ and a decoder function $g : \mathcal{Z} \rightarrow \mathcal{X}$ that solves the following fair empirical representation problem

$$\min_{t, g} \mathcal{L}_{rec}(g, t, \mathcal{D}_n) \text{ subject to } \Delta_n(t) \leq \delta, \quad (4)$$

where $\delta > 0$ is a pre-specified demographic parity threshold and \mathcal{L}_{rec} is a reconstruction loss whose choice depends on the data.

2.2 Necessary Condition

This section identifies a necessary condition on deterministic representation mapping t for the induced empirical demographic parity certificate to approximate $\Delta^*(t)$ well. The necessary condition bounds the amount of information measured by the χ^2 mutual information between feature X and representation Z :

$$I_{\chi^2}(X, Z) \triangleq E_x E_z \left(\frac{\mu_t(z) - \mu_t(Z|X=x)}{\mu_t(z)} \right)^2. \quad (5)$$

The χ^2 mutual information relies on a statistical distance, the χ^2 -divergence

$$\chi^2(Z, Z|X) = \int_z (dP(Z|X)/dP(Z) - 1)^2 dP(Z)$$

to average the distance between Z and $Z|X = x$ for $x \in \mathcal{X}$. It has been used in information theory to estimate the information that flows through a neural network (see [10]). In the context of fair representation learning, we find that empirical demographic parity certificates cannot provide good approximations of the representation's true demographic parity if the χ^2 input-output mutual information is large:

Theorem 2.1. *Let $n \geq 1$. Consider a representation function $t : \mathcal{X} \rightarrow \mathcal{Z}$. Then,*

$$\inf_{f_n \in \mathcal{F}_n} \sup_{\mu} E_{\mathcal{D}_n} |\Delta^*(t) - \Delta(f_n, t)| - \left(1 - \frac{1}{I_{\chi^2}(X, Z)} \right)^n \geq 0. \quad (6)$$

We prove the result in Theorem 2.1 for any representation function and conjecture, but have not proved it, that it still holds true for any representation mapping. Encoding more information of X in Z exposes the representation distribution μ_t to mirroring distributions over \mathcal{X} with heavy tails. Intuitively, μ_t is a (possibly infinite) mixture of conditional distributions $P(Z|X = x)$ for $x \in \mathcal{X}$ and $I_{\chi^2}(X, Z)$ measures an average distance between those conditional distributions. As $I_{\chi^2}(X, Z)$ increases, the conditional distributions $P(Z|X = x)$ become far apart for a growing mass of $x \in \mathcal{X}$. It generates a representation distribution too complex for a finite sample to represent it and for an auditor f_n to detect all the correlations between representation and sensitive attribute.

Theorem 2.1 implies a trade-off between the information passed from feature to representation and the approximation rate of empirical demographic parity certificates:

Corollary 2.1. *With the notations from Theorem 2.1, suppose that*

$$\inf_{f_n \in \mathcal{F}_n} \sup_{\mu} E_{\mathcal{D}_n} |\Delta^*(t) - \Delta(f_n, t)| \leq \epsilon_n,$$

then for all distributions over the feature space \mathcal{X} ,

$$I_{\chi^2}(X, Z) \leq \frac{1}{1 - \epsilon_n^{\frac{1}{n}}}. \quad (7)$$

The smaller the approximation rate ϵ_n is, the smaller is the upper bound on the χ^2 -mutual information between X and Z . For the approximation rate of $\Delta^*(t) - \Delta(f_n, t)$ to be $O(n^{-s})$ for some $s > 0$, it is necessary for the χ^2 mutual information between feature and representation to be bounded above by $O(n/(s \ln(n)))$ for *all* distributions over \mathcal{X} . On the other hand, representation functions t for which the χ^2 mutual information is infinite for some distribution over the features space, never guarantee a meaningful approximate rate between $\Delta^*(t)$ and $\Delta_n(f_n, t)$ for any auditor f_n :

Corollary 2.2. *Let $n \geq 1$. Consider a representation function $t : \mathcal{X} \rightarrow \mathcal{Z}$. Suppose that there exists a distribution over \mathcal{X} such that $I_{\chi^2}(X, Z) = \infty$. Then,*

$$\inf_{f_n \in \mathcal{F}_n} \sup_{\mu} \Delta^*(t) - \Delta(f_n, t) \geq 1. \quad (8)$$

Examples: The results in corollary 2.1 and 2.2 imply that empirical certificates of representation distributions induced by many common encoders do not have meaningful approximation rates:

- Suppose that t is injective from \mathbb{R}^D to \mathbb{R}^d . Then, there exists a distribution over $\mathcal{X} \times \{0, 1\}$ such that $I_{\chi^2}(X, Z) = \infty$ and thus, $\Delta^*(t) = 1$, but $\Delta(f_n, t) = 0$ for all auditing functions f_n .
- Suppose that $|\{t(x)|x \in \mathcal{X}\}| \geq n/(\ln(n))^\alpha$, for some $\alpha < 1$. Then, the approximation rate of $\Delta(f_n, t)$ for all auditing functions f_n is $\omega(n^{-s})$ for any $s > 0$.

2.3 Sufficient Condition

This section shows that a finite χ^2 mutual information between feature and representation for all distributions over \mathcal{X} is a sufficient condition for empirical demographic parity certificates to converge at a $O(n^{-1/2})$ rate.

Theorem 2.2. *Let $n \geq 1$. Consider a representation mapping $t : \mathcal{X} \rightarrow \mathcal{Z}$. Then, if \mathcal{F}_n denotes the set of all auditors $f_n : \mathcal{Z} \times (\mathcal{Z} \times \{0, 1\})^n \rightarrow \{0, 1\}$, if $n_s = |\{i|s_i = s\}|$,*

$$\begin{aligned} & \inf_{f_n \in \mathcal{F}_n} \sup_{\mu} E_{\mathcal{D}_n} |\Delta^*(t) - \Delta(f_n, t)| \\ & - 2 \sum_{s=0,1} n_s^{-1/2} \sqrt{I_{\chi^2}(X, Z|S=s)} \leq 0 \end{aligned} \quad (9)$$

A finite χ^2 mutual information between X and Z implies that $P(Z)$ and $P(Z|X)$ are close in the sense of the χ^2 divergence and thus by sampling representations from $P(Z|X)$, we have a non-zero probability to sample all the atoms that can form the representation distribution μ_t and thus to detect all the dependence between representations and sensitive attributes.

2.4 χ^2 versus Classic Mutual Information

Our results in Theorems 2.1 and 2.2 highlight the connection between the χ^2 mutual information and the approximation rate of empirical certificates. A similar result cannot be obtained with the classic mutual information $I_{Sh}(X, Z)$ that is based on Shannon entropy.

To demonstrate this point, we construct the following distribution μ over $\mathcal{X} \times \{0, 1\}$. Features are uniformly distributed over $[0, 1]$ and $t(x) = i$ for $x \in [1/i, 1/(i+1))$ and $i > 0$. For each $i > 0$, the sensitive attribute is constant over $[1/i, 1/(i+1))$ and equal to 1 with probability 1/2. We show in the appendix that $I_{Sh}(X, Z) < \ln(6)/3 + 3$, but $I_{\chi^2}(X, Z) = \infty$. Since the sensitive attribute S is a deterministic function of the representation $Z = t(X)$, $\Delta^*(t) = 1$. But, for a finite sample of size n , $E_{\mathcal{D}_n} \Delta(f_n, t)$ is zero for all auditors f_n , despite $I_{Sh}(X, Z) < \infty$.

3 Smooth and Fair Representations

The previous section suggests restricting the fair representation problem (4) to representation mappings for which the χ^2 mutual information between feature and representation is finite for all distributions over \mathcal{X} . In this section, this sufficient condition is met by introducing an additive Gaussian white noise (AWGN) channel after the encoder t .

3.1 Convergence of Smoothed Empirical Certificate

For any representation mapping $t : \mathcal{X} \rightarrow \mathcal{Z}$, we denote t_σ the convolution of t with a Gaussian noise $\mathcal{N}(0, \sigma^2 I_d)$: $t_\sigma(X) = t(X) + noise$, with $noise \sim \mathcal{N}(0, \sigma^2 I_d)$. The convolved representation $Z_\sigma = Z + noise$ has a distribution denoted $\mu_{t*\sigma}$. The convolution smoothes the representation distribution by making $P(Z_\sigma|X)$ a Gaussian whose support covers the support of the representation distribution $P(Z)$ and thus, guarantees that samples from different conditional distributions $P(Z_\sigma|X=x)$ are not too far away.

Theorem 3.1. *Let $\sigma > 0$ and $n \geq 1$. For all representation mapping $t : \mathcal{X} \rightarrow \mathcal{Z}$ and for any distribution over \mathcal{X} , if $\|t\|_\infty \triangleq \sup_{x \in \mathcal{X}} \|t(x)\|_2$, then for $s \in \{0, 1\}$*

$$I_{\chi^2}(X, Z|S=s) \leq \exp\left(\frac{\|t\|_\infty^2}{\sigma^2}\right) < \infty. \quad (10)$$

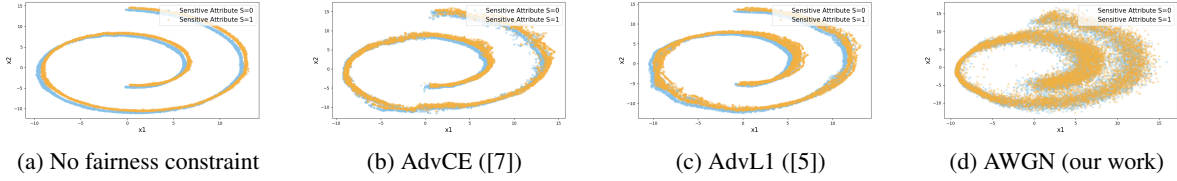


Figure 2: **Without additional guarantees, fair representation learning could still leak information related to sensitive attribute.** This visualizes in a 2D-plane representations from the Swiss Roll data set once passed through a decoder. The easier it is to visually distinguish sensitive attributes, the more information related to sensitive attribute the representation leaks.

Therefore,

$$\begin{aligned} & \inf_{f_n \in \mathcal{F}_n} \sup_{\mu} E_{\mathcal{D}_n} [\Delta^*(t_\sigma) - \Delta(t_\sigma, f_n)] \\ & \leq 2 \exp\left(\frac{\|t\|_\infty^2}{2\sigma^2}\right) (n_0^{-1/2} + n_1^{-1/2}). \end{aligned} \quad (11)$$

The upper bound in Theorem 3.1 does not depend on the dimensions d of the representation space \mathcal{Z} , but only on $n^{-1/2}$ and on the ratio $\|t\|_\infty/\sigma$ that can be interpreted as a signal-to-noise ratio in the AWGN channel. Larger values of $\|t\|_\infty$ increase the variance of Z and thus require larger noise σ to keep the conditional distribution $P(Z_\sigma|X)$ close to the distribution $P(Z_\sigma)$. The bound is only meaningful if $\|t\|_\infty < \infty$, which holds, for example, if the features space is bounded and t is a continuous mapping.

Both Theorems 2.2 and 3.1 rely on a plug-in auditor that first estimates the class-conditional densities $\mu_{t^*\sigma}^0$ and $\mu_{t^*\sigma}^1$. From a sample $\mathcal{D}_n = \{(x_i, s_i)\}_{i=1}^n$, we construct an empirical estimate of $\mu_{t^*\sigma}$ over $\mathcal{Z} \times \{0, 1\}$ as

$$\mu_{n,\sigma}(z, s) = \sum_{i=1, s_i=s}^n P(z|X = x_i) \quad (12)$$

with $P(\cdot|X = x_i) \sim \mathcal{N}(t_n(x_i), \sigma I_d)$. Our plug-in auditor f_n^{plug} compares $\mu_{n,\sigma}(z, 0)$ to $\mu_{n,\sigma}(z, 1)$:

$$f_n^{plug}(z) = \begin{cases} 0 & \text{if } \mu_{n,\sigma}(z, 0) \geq \mu_{n,\sigma}(z, 1) \\ 1 & \text{otherwise.} \end{cases} \quad (13)$$

Since we obtain the upper bounds in Theorems 2.2 and 3.1 with the plug-in auditor f_n^{plug} , we can guarantee that the representation demographic parity is within $O(n^{-1/2})$ of the empirical certificate signed by the plug-in auditor.

3.2 Learning Fair Representation

In practice, the representation mapping t and the decoder g are modelled by neural networks. An AWGN channel is added to t to learn a smoothed representation distribution $\mu_{t^*\sigma}$. The data controller trades off minimizing a reconstruction loss $\mathcal{L}_{rec}(t, g) = E_x[l_{rec}(t, g, x)]$ with minimizing demographic unparity $\mathcal{L}_{DP}(t) = \Delta^*(t_\sigma)$. With a sample $\mathcal{D}_n = \{(x_i, s_i)\}_{i=1}^n$, the data controller uses the plug-in auditor and solves the empirical minimization problem as

$$\min_{t,g} \frac{1}{n} \sum l_{rec}(t, g, x_i) + \lambda \Delta(f_n^{plug}, t_\sigma), \quad (14)$$

where λ controls for the strength of the fairness constraint imposed on the representation distribution. The minimization problem in (14) differs from previous work on fair representation learning because of the noise added to Z . The main advantage of convolving the representation distribution with a Gaussian noise is that the finite-sample fairness constraint $\Delta(f_n^{plug}, t_\sigma)$ approximates $\Delta^*(t_\sigma)$ at a rate $O(n^{-1/2})$, while previous work does not offer this guarantee (see section 2).

The second advantage is that the empirical demographic parity certificate can be computed without modelling the auditor by an additional neural network. This is because we can use our empirical estimates (38) of the class-conditional densities to estimate the posterior distribution $\eta(z, s) = P(S = s|Z = z)$ as $\eta_n(z, s) = \mu_{n,\sigma}(z|S = s)/\mu_{n,\sigma}(z)$, where $\mu_{n,\sigma}(z) = \mu_{n,\sigma}(z, 1) + \mu_{n,\sigma}(z, 0)$. Since $\Delta^*(t)$ relates to the balanced error rate of predicting the sensitive attributes (see proof of 2.2 or [15]), we can write $\Delta^*(t) = \mathcal{L}_{DP}(\mu_{t,\sigma})$, where $\mathcal{L}_{DP}(\mu_{t,\sigma}) = E_{z \sim \mu_{t,\sigma}}[|\eta(z, 1) - \eta(z, 0)|]$ (see

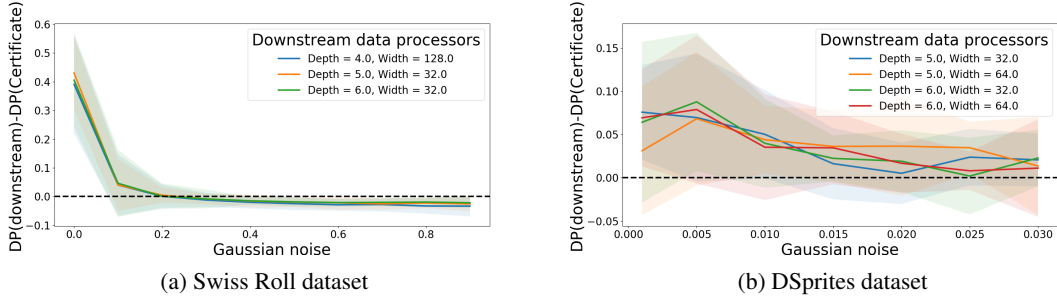


Figure 3: **Generalization properties of empirical demographic parity certificates obtained by adding an additive Gaussian white noise (AWGN) channel to fair representation learning.** This shows the difference between the demographic parity measured by the empirical certificate and the one obtained by downstream processors that attempt to predict the sensitive attribute while observing fresh samples from the representation distribution. Differences below the horizontal dashed line indicate that the empirical certificate is a reliable approximation of the demographic parity of the representation distribution. Shaded areas captures the one standard deviation around the median of 100 simulations.

[30]). Our approach relies on two results: (i) for any finite sample of size n , $\mathcal{L}_{DP}(\mu_{n,\sigma})$ approximates well $\mathcal{L}_{DP}(\mu_{t^* \sigma})$; (ii) $\mathcal{L}_{DP}(\mu_{n,\sigma})$ can be estimated efficiently by Monte-Carlo estimation. The first observation uses the following result, which is a consequence of Theorem 3.1

Theorem 3.2. *Let $\sigma > 0$ and $n \geq 1$. For all representation mapping $t : \mathcal{X} \rightarrow \mathcal{Z}$*

$$\begin{aligned} & \sup_{\mu} E_{\mathcal{D}_n} |\mathcal{L}_{DP}(\mu_{t^* \sigma}) - \mathcal{L}_{DP}(\mu_{n,\sigma})| \\ & \leq 2 \exp\left(\frac{\|t\|_{\infty}^2}{2\sigma^2}\right) (n_0^{-1/2} + n_1^{-1/2}). \end{aligned} \quad (15)$$

Therefore, we can use $\mathcal{L}_{DP}(\mu_{n,\sigma})$ as an approximation of $\mathcal{L}_{DP}(\mu_{t^* \sigma})$. That is, in place of $\mu_{t,\sigma}$, we propose to use the distribution $\mu_{n,\sigma}$, for which η_n is the posteriori probability. Moreover, $\mathcal{L}_{DP}(\mu_{n,\sigma})$ can be efficiently approximated by Monte Carlo integration. For a sample of features $\mathcal{D}_n = \{(x_i, y_i)\}_{i=1}^n$, $\mu_{n,\sigma}^0$ and $\mu_{n,\sigma}^1$ are mixtures of d -dimensional Gaussians. Thereby, we approximate $\mathcal{L}_{DP}(\mu_{n,\sigma})$ with

$$\hat{\mathcal{L}}_{DP}(\mu_{n,\sigma}) = \frac{1}{nm} \sum_{i=1}^n \sum_{j=1}^m E_{\epsilon} [|\eta_n(z_{ij}, 1) - \eta_n(z_{ij}, 0)|], \quad (16)$$

where $z_{ij} = t(x_i) + noise_{ij}$, $\{noise_{ji}\}$ is a vector of $n \times m$ draws from a d -dimensional Gaussian $\mathcal{N}(0, \sigma I_d)$ and m is the number of draws per sample point. $\hat{\mathcal{L}}_{DP}(\mu_{n,\sigma})$ is an unbiased approximation of $\mathcal{L}_{DP}(\mu_{t,\sigma})$ and achieves a Mean-Squared-Error (MSE) of order $O(n^{-1}m^{-1})$ (see proof of Theorem 4 in appendix).

To sum up, the data controller learns (t, g) by minimizing the following combined empirical loss

$$\min_{\theta, \varphi} \frac{1}{n} \sum_i l_{rec}(t, g, x_i) + \lambda \hat{\mathcal{L}}_{DP}(\mu_{n,\sigma}). \quad (17)$$

Practical implementation. We minimize the loss (17) by stochastic gradient descent. Each mini-batch is split in half: the first half is used to estimate $\mu_{n,\sigma}$ as in (38); the second half to estimate the loss in (17) with $m = 1$. At the end of training, we compute a leave-one-out balanced error rate $BER(f_n^{plug})$ for the plug-in auditor on both a test and train samples and infer an empirical certificate as $\Delta(f_n^{plug}, t) = 1 - 2BER(f_n^{plug})$ (see [15]). The Gaussian noise σ is an hyper-parameter chosen so that empirical certificate estimated on train and test data are similar.

4 Experiments

4.1 Synthetic Datasets

Our first synthetic data consists of two 3D Swiss rolls: one for $S = 0$ and one shifted South-West for $S = 1$ (see 2a). We use 20,000 samples for training the autoencoder (t, g) and 10,000 fresh samples to train the downstream test

functions. The autoencoder is a neural network with seven hidden layers and 32 neurons each with RELU activation and is trained with a learning rate of 0.001 for 400 epochs. The value of the fairness coefficient λ in (17) is 5. The representation space has dimension 3 ($d = 3$).

Our second synthetic data is a variant of the DSprites dataset ([31]) that contains 64 by 64 black and white images of various shapes (heart, square, circle). Since fair representation mapping consists of disentangling sensitive attributes from the rest of the features, DSprites offers an interesting challenge ([6]). The DSprites dataset has six independent factors of variation: color (black or white); shape (square, heart, ellipse), scales (6 values), orientation (40 angles in $[0, 2\pi]$); x- and y- positions (32 values each). We adapt the sampling to generate a source of potential unfairness. We consider shape as the sensitive attribute. Following [6], we assign to each possible combination of attributes a weight proportional to $\frac{i_{shape}}{3} + \left(\frac{i_X}{32}\right)^3$, where $i_{shape} \in \{0, 1, 2\}$ and $i_X = \{0, 1, \dots, 21\}$. Then, we sample 60,000 combinations of the six factors of variations according to the weights. We use 50,000 samples to train the autoencoder and 10,000 to train the downstream test functions. The autoencoder architecture – borrowed from [6] – includes 4 convolutional layers and 4 deconvolutional layers and uses RELU activation. The model is trained with a learned rate of 0.0001 for 400 epochs. The value of the fairness coefficient λ in (17) is 0.2. The dimension of the representation space is 10.

Effect of noise on certificate reliability. For both datasets, we first learn an encoder-decoder mapping (t, g) with an increasing amount of Gaussian noise; estimate an empirical $\Delta(f_n^{plug}, t)$ —demographic parity certificate; and then, test whether $\Delta(f_n^{plug}, t)$ is larger than the demographic parity $\Delta(f, t)$ of different downstream test functions f . Our test functions predict sensitive attributes from new samples of the representation distribution. We model them as fully connected neural networks with 4 to 6 hidden layers with 32 to 128 neurons each. Each test function is trained for 400 epochs with a learning rate of 0.001. After the autoencoder is trained, its weights are frozen, and fresh representations are generated by 10,000 forward passes of the encoder on the test data. The generated fresh representations form the inputs of the test functions.

Figure 3 shows that the AWGN channel improves how empirical certificates approximate the demographic parity of the representation distribution. As the Gaussian noise σ increases, the difference between the demographic parity of downstream test functions and of the empirical certificate decreases. For the Swiss Roll dataset (see Figure 3a), with $\sigma^2 > 0.1$, the $\Delta(f_n^{plug}, t)$ empirical certificate upper bounds the demographic parity of any of the downstream test functions we built, regardless of their complexity. For the DSprites dataset, the empirical certificate approximates better the demographic parity obtained by the downstream test functions for $\sigma^2 > 0.02$ (see Figure 3b). Moreover, the variance of $\Delta(f_n, t) - \Delta(f, t)$ decreases as the Gaussian noise increases. This is consistent with the upper bound in Theorem 3.1, which decreases with smaller signal-to-noise ratio $\|t\|_\infty/\sigma$.

Comparative adversarial approaches. We benchmark the use of an AWGN channel with comparative approaches in fair representation learning based on an adversarial auditor (*AUD*) trained with (i) a cross-entropy loss (AdvCE, [7]); or, with (ii) a group L1 loss (AdvL1, [5]).

AdvCE is a fair representation learning method from [7]. The auditor is modeled as an adversarial neural network f that predicts sensitive attributes from samples of the representation distribution and minimizes the following cross-entropy loss:

$$\mathcal{L}_{CE}(f) = -\frac{1}{n} \sum_{i=1}^n s_i \log(f(x_i)) + (1 - s_i) \log(1 - f(x_i)). \quad (18)$$

Moreover, the autoencoder is trained to minimize a loss $\mathcal{L}_{rec} - \lambda \mathcal{L}_{CE}(f)$.

AdvL1 ([5]) replaces the cross-entropy loss by a group L1 loss: instead of (18), the adversary minimizes

$$\mathcal{L}_{L1} = \frac{1}{n_0} \sum_{i, s_i=0} f(x_i) - \frac{1}{n_1} \sum_{i, s_i=1} f(x_i), \quad (19)$$

and the autoencoder minimizes $\mathcal{L}_{rec} - \lambda \mathcal{L}_{L1}(f)$.

For both AdvCE and AdvL1, the autoencoder is the same as in the experiments in Figure 3. The adversarial auditor is modeled as a neural network with seven hidden layers of 32 neurons each. For both Swiss Roll and DSprites, the autoencoder is trained for 400 epochs with a learning rate of 0.0001; the adversary with a learning rate of 0.001. For Swiss Roll, the fairness coefficient λ is 20 for both AdvCE and AdvL1 and 5 for AWGN; for DSprites, λ is 0.1 for both AdvCE and AdvL1 and 0.15 for AWGN. The downstream processor (*PROC*) stacks the (frozen) layers of the decoder g with 4 hidden neural layers of a fully connected network. Crucially for our experiment, the decoder does not use any information related to sensitive attribute.

Table 1 measures the performance of empirical certificates as the difference $PROC - AUD$ between the unparity measured by *PROC* and *AUD*: the lower the difference, the more reliable is the empirical certificate. For both

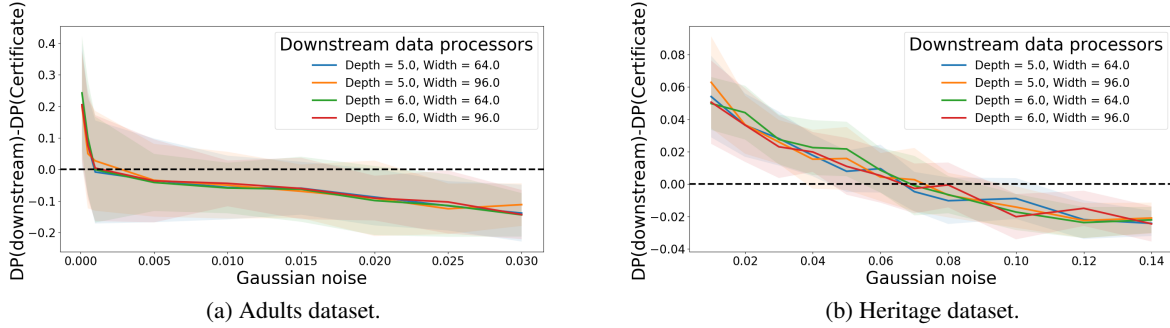


Figure 4: **Generalization properties of empirical demographic parity certificates obtained by adding an additive Gaussian white noise (AWGN) channel to fair representation learning.** See Figure 3.

comparative methods, the adversarial auditor AUD estimates the representation distribution to be almost independent of sensitive attribute – auditor’s demographic parity is almost zero, but our downstream processor $PROC$ predicts with high accuracy the sensitive attribute and thus, has much higher demographic parity (0.8 for Swiss Roll and 0.4 – 0.5 for DSprites). On the other hand, the introduction of an AWGN channel reduces the difference $PROC - AUD$ and guarantees that the empirical certificate estimated by the auditor AUD approximates well the demographic parity of the downstream processor $PROC$. However, for the Swiss Roll dataset, a better approximation comes at the cost of a higher $L2$ – reconstruction loss.

Table 1: **Robustness of fair representation learning:** This table compares for both Swiss Roll (SW) and DSprites (DS) datasets the use of an AWGN channel (AWGN) with alternative fair representation learning methods that use adversarial auditors with cross-entropy loss (**AdvCE**, [7]) or group L1 loss (**AdvL1**, [5]). The lower the difference $PROC-AUD$ between processor’s ($PROC$) and auditor’s (AUD) measure of unparity, the better empirical certificates approximate the representation’s demographic parity. Results are the median of 100 simulations for each method.

DATASET	MODEL	L2 Loss	MEASURED UNPARITY		
			AUD	PROC	PROC-AUD
SW	ADVCE	0.09	0.05	0.79	0.74
SW	ADVL1	0.02	0.04	0.8	0.76
SW	AWGN	1.19	0.08	0.13	0.05
DS	ADVCE	0.01	0.02	0.54	0.52
DS	ADVL1	0.01	0.06	0.39	0.33
DS	AWGN	0.01	0.14	0.2	0.06

Visually, Figure 2 shows one of our simulation results for the Swiss Roll dataset and compares the representations generated by each comparative method and decoded by the downstream processor $PROC$. Although the three fair learning methods, AdvCE, AdvL1 and ours AWGN, certify the representation distribution to be almost independent of sensitive attribute, only the AWGN approach makes it really difficult to distinguish the sensitive attributes when looking at the decoded representation.

4.2 Application to Fair ML benchmark datasets

We apply our approach of fair representation learning with a AWGN channel to two fair learning benchmarks, Adults¹ and Heritage². The Adults dataset contains 49K individuals and includes information on 10 features related to professional occupation, education attainment, race, capital gains, hours worked and marital status. The sensitive attribute is the gender to which individuals self-identify to. The data is split into a 34K train set and a 15K test set.

The Health Heritage dataset contains 220K individuals with 66 features related to age, clinical diagnoses and procedure, lab results, drug prescriptions and claims payment aggregated over 3 years. The sensitive attribute is the gender to which individuals self-identify to. After removing individuals with missing records, we split the data into a 142K/35K train/test split.

¹<https://archive.ics.uci.edu/ml/datasets/adult>

²<https://foreverdata.org/1015/index.html>

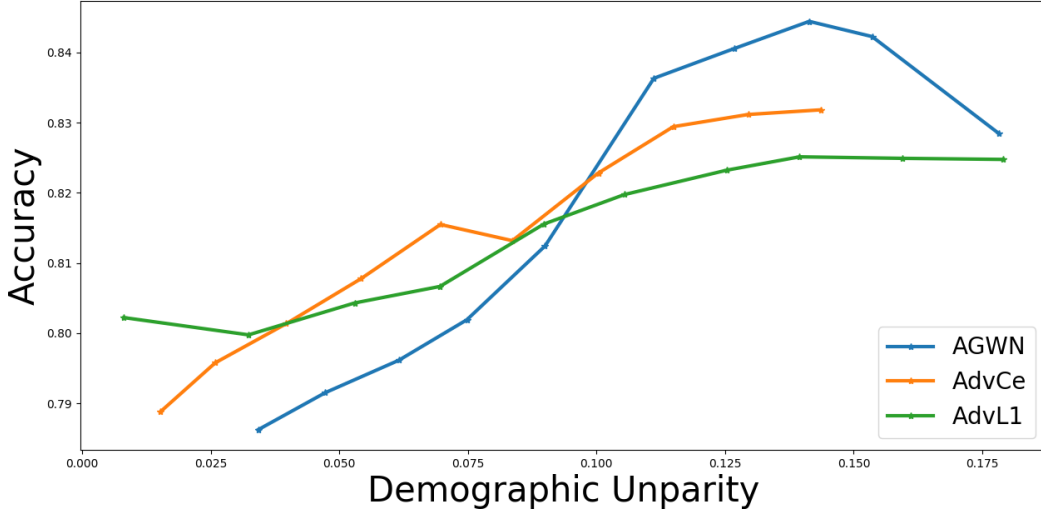


Figure 5: **Pareto Front for fair representation learning approaches.** This shows an accuracy-fairness trade-off by measuring the accuracy and the demographic parity of neural networks of various depth and width that detect wealthy individuals from representations of the Adult dataset.

For both Adults and Heritage the autoencoder has seven hidden layers of 32 neurons each and is trained for 400 epochs with a learning rate of 0.0005. The dimension of the representation latent space is 10 for Adults and 24 for Heritage. The fairness coefficient λ is 3 for Adults and 0.5 for Heritage. Downstream test functions are trained as in Figure 3.

Effect of noise on certificate reliability. In Figure 4, downstream data processors probe the demographic parity of the learned representation distribution by predicting the gender of representations encoded from a test sample of 15K individuals for Adults and 35K individuals for Heritage. As in Figure 3, we compare the demographic parity of these downstream processors to the empirical certificate estimated after training. For both datasets, Figure 4 confirms that (i) without the noisy channel (small σ), the empirical certificate underestimates the demographic unparity of downstream data processors; but, (ii) that the AWGN channel is sufficient for empirical certificates to upper-bound the demographic unparity obtained by various downstream users.

Accuracy-fairness trade-off. To explore how the AWGN channel affects the information contained in the representation distribution, we retrain on the Adults dataset the three fair learning methods – AdvCE, AdvL1 and AWGN – but leave out the feature related to income. We generate from the test samples their corresponding representations and predict whether their income is over 50K.

We construct Pareto fronts (see [5]) by sweeping the parameter space for values of the fairness coefficient λ between 0 and 4 and by training for each value of λ an autoencoder for the three comparative methods, AdvCE, AdvL1 and AWGN. The AWGN channel uses a noise σ of 0.015. Both adversarial methods use auditors modeled as neural networks with six hidden layers that are trained with a learning rate of 0.005. After we train the autoencoder, we freeze its weights, generate fresh samples from the representation distribution using the test data of 15K individuals, and predict whether an individual earns more than 50K a year. We apply this downstream task to four classifiers that we model as neural networks of depth varying from 3 to 6. We repeat the simulation 10 times and thus obtain 40 demographic parity/accuracy tuples for each value of λ and each of the three fair representation learning methods (AdvCE, AdvL1 and AWGN). We bin the demographic parity values in 10 buckets and report 75%– quantile accuracy attained within each bin.

The resulting Pareto fronts in Figure 5 show that compared to alternative fair learning methods, the AWGN channel does not appear to degrade significantly the accuracy-fairness trade-off: the trade-off is worse at low level of demographic parity and better at higher level of demographic parity. Although the AWGN channel limits the maximum amount of information that is transferred from the data to the representation (see [32]), it also allows for a better empirical approximation of demographic parity and thus helps guiding the representation mapping toward the correct fairness-information trade-off.

5 Conclusion

This paper investigates whether a data controller could generate representations of the data with fairness guarantees that would hold for any downstream processor using samples from the representation distribution. We show that for demographic parity certificate to approximate well the demographic parity of all future data processors it is necessary and sufficient to bound the χ^2 mutual information between feature and representation. To meet this condition, we show the benefit of adding an AWGN channel while learning a fair representation of the data.

Our work opens promising research avenues in fair representation learning. An AWGN channel may be only one of many approaches to bound the χ^2 mutual information between feature and representation. A comparison of competitive approaches would be crucial to improve the accuracy-fairness trade-off of learning reliably fair representations.

6 Appendix - Proofs of Results

6.1 Proof of Theorem 2.1

The proof of Theorem 2.1 uses the following lemma (from [15]) that links the demographic parity of a test function f and its balanced error rate $BER(f)$,

$$BER(f, t) = \frac{P(f(Z) = 1|S = 0) + P(f(Z) = 0|S = 1)}{2}, \quad (20)$$

where we make the dependence on the representation mapping t explicit in $BER(f, t)$.

Lemma 6.1. [15] *A representation space (\mathcal{Z}, μ_t) satisfies an $\Delta^*(t)$ -demographic parity certificate if and only if*

$$BER^*(t) \triangleq \min_{f: \mathcal{Z} \rightarrow \{0,1\}} BER(f, t) \geq \frac{1 - \Delta}{2}. \quad (21)$$

Therefore, a representation space (\mathcal{Z}, μ_t) can be stamped with a $\Delta^(t)$ -demographic parity certificate with $\Delta^*(t) \equiv 1 - 2BER^*(t)$.*

To prove the result in Theorem 2.1, we consider a distribution μ over $\{1, 1/2, 1/3, \dots\}$ and assume that t is deterministic. Therefore, since t is deterministic, the representation distribution induced by t is discrete and can be indexed by k . We denote $t(\mathcal{X}) = \{z_1, z_2, \dots, z_K\}$, with $K \leq \infty$ and $z_k \neq z_{k'}$ for $k \neq k'$. In this setting, the χ^2 mutual information has an analytical form:

Lemma 6.2. *Suppose that t is a deterministic mapping from \mathcal{X} to \mathcal{Z} . Assume that $t(\mathcal{X}) = \{z_1, z_2, \dots, z_K\}$ with $K \leq \infty$ and $z_k \neq z_{k'}$ for $k \neq k'$. Then, for all distribution over the features \mathcal{X} such that $P(t(X) = z_k) > 0$, $I_{\chi^2}(X, Z) = K - 1$.*

Proof. First, since t is a function, $P(Z = z_k|X = x)$ is equal to one if and only if $t(x) = z_k$. Therefore,

$$\begin{aligned} I_{\chi^2}(X, Z) &= E_x \left(1 - \frac{1}{P(Z = t(x))} \right)^2 P(Z = t(x)) \\ &= E_x \left[\frac{1}{P(Z = t(x))} \right] - 1 \\ &= \sum_{k=1}^K \left[\frac{P(X, t(X) = z_k)}{P(Z = z_k)} \right] - 1 \\ &= K - 1 \end{aligned} \quad (22)$$

□

For each $k \in \{1, \dots, K\}$, we choose one $x_k \in \mathcal{X}$ such that $t(x_k) = z_k$. We parametrize a family of joint distributions $\mu(b)$ over $[0, 1] \times \{0, 1\}$ as follows: X is uniformly distributed over $\{x_1, \dots, x_K\}$; and, for $b \in (0, 1)$, the sensitive attribute is given by k^{th} binary expansion of b , where $X = x_k$. By Lemma 6.3, the χ^2 squared mutual information between X and $t(X)$ is the same for any b and equal to $K - 1$. Moreover, since the sensitive attribute is a function of $t(X)$, $\Delta_b^*(t) = 1$, where the subscript indicates that demographic parity is computed using the joint distribution $\mu(b)$ over (Z, S) .

Let B denote a random variable uniformly distributed on $[0, 1]$. For any auditor f_n ,

$$\begin{aligned}
\sup_{b \in [0,1]} E_{\mathcal{D}_n(b)} \text{BER}(f_n, t) &\stackrel{(a)}{\geq} E_B E_{\mathcal{D}_n(B)} \text{BER}(f_n, t) \\
&= E_{X,B} P[f_n((t(X), \mathcal{D}_n(B)) \neq \\
&\quad S | t(X_1), \dots, t(X_n), S_1, \dots, S_n, t(X))] \\
&\stackrel{(b)}{\geq} \frac{1}{2} P(\cap_{i=1}^n [t(X) \neq t(X_i)]) \\
&\stackrel{(c)}{=} \frac{1}{2} \left(1 - \frac{1}{K}\right)^n \\
&\stackrel{(d)}{=} \frac{1}{2} \left(1 - \frac{1}{I_{\chi^2}(X, Z)}\right)^n
\end{aligned} \tag{23}$$

where (a) uses that the supremum is larger than the average; (b) that for $Z \notin \{Z_1, \dots, Z_n\}$, the sensitive attribute has a Bernoulli distribution with probability $1/2$; (c) that X and then Z is uniformly distributed; and, (d) that $I_{\chi^2}(X, Z) \leq K$ by Lemma 6.2. Since $I_{\chi^2}(X, Z)$ is equal for all b , it follows from Lemma 6.1 that

$$\sup_{b \in (0,1)} \Delta^* - \Delta(f_n, t) \geq \left(1 - \frac{1}{I_{\chi^2}(Z, X)}\right)^n. \tag{24}$$

Therefore, there exists a distribution μ over $\mathcal{X} \times \{0, 1\}$ such that for all auditors f_n ,

$$E_{\mathcal{D}_n} |\Delta^* - \Delta(f_n, t)| \geq \left(1 - \frac{1}{I_{\chi^2}(Z, X)}\right)^n. \tag{25}$$

6.2 Proof of Corollary 2.1

Suppose that $\inf_{f_n \in \mathcal{F}_n} \sup_{\mu} E_{\mathcal{D}_n} |\Delta^* - \Delta(f_n, t)| \leq \epsilon_n$ for some $\epsilon_n > 0$. Let $f_n \in \mathcal{F}_n$ be the auditor that reaches the minimum.

We have, for any distribution μ over $\mathcal{X} \times \{0, 1\}$,

$$\begin{aligned}
\left(1 - \frac{1}{I_{\chi^2}(Z, X)}\right)^n &\leq \sup_{\mu} \left(1 - \frac{1}{I_{\chi^2}(Z, X)}\right)^n \\
&\stackrel{(a)}{\leq} \sup_{\mu} E_{\mathcal{D}_n} |\Delta^* - \Delta(f_n, t)| \\
&\leq \epsilon_n,
\end{aligned} \tag{26}$$

where (a) uses Theorem 2.1. The result follows directly from equation (26).

6.3 Proof of Corollary 2.2

We first show the following Lemma:

Lemma 6.3. *Let t be a function from \mathcal{X} to \mathcal{Z} . Suppose that there exists a distribution μ over $\mathcal{X} \times \{0, 1\}$ such that $I_{\chi^2}(X, Z) = \infty$. Then, there exists an infinite countable set $\{a_k\}$ of \mathcal{X} such that for all $k \neq k'$, $t(a_k) \neq t(a_{k'})$.*

Proof. The proof proceeds by contradiction. Assume that we have a partition $t(\mathcal{X}) = \{a_k\}_{k=1}^M$ for a fixed $M < \infty$. Given that t is a function, as in the proof of Lemma 6.2,

$$\begin{aligned}
\infty = I_{\chi^2}(X, Z) &= E_x \left[\frac{1}{P(Z = t(x))} \right] - 1 \\
&= \sum_{k=1}^M \frac{\mu(\{x | t(x) = a_k\})}{P(t(X) = t(a_k))} - 1 \\
&\stackrel{(a)}{=} M,
\end{aligned} \tag{27}$$

where (a) uses the fact that $\mu(\{x|t(x) = a_k\}) = P(t(X) = t(a_k))$. Equation (27) contradicts $M < \infty$. \square

Therefore, by Lemma 6.3, if for a distribution μ over $\mathcal{X} \times \{0, 1\}$, $I_{\chi^2}(Z, X) = \infty$, then there exists an infinite countable set $\{a_k\}$ of \mathcal{X} such that t takes a different value at each a_k . We choose X to take value in $\{a_k\}_{k \geq 1}$ such that $P(a_k) = p_k$ for $k \geq 0$ where the sequence $\{p_k\}_{k=1}^{\infty}$ will be chosen later on. As in the proof of Theorem 2.1, we parametrize a family of distributions over $\mathcal{X} \times \{0, 1\}$ by $b \in (0, 1)$ such that for $X \in \{a_1, \dots\}$, the sensitive attribute S is the k^{th} term of b 's binary expansion, where $X = a_k$. Because S is a deterministic function of X , $\Delta^*(t) = 1$.

Let B denote a random variable uniformly distributed on $[0, 1]$. The rest of the proof follows the same steps as in the proof of Theorem 2.1. For a sample point X_i , we denote k_i such that $X_i = a_{k_i}$. For any auditor f_n ,

$$\begin{aligned} \sup_{b \in [0,1]} E_{\mathcal{D}_n(b)} \text{BER}(f_n, t) &\stackrel{(a)}{\geq} E_B E_{\mathcal{D}_n(B)} \text{BER}(f_n, t) \\ &= E_{X,B} P[f_n(t(X), \mathcal{D}_n(B)) \neq \\ &\quad S | t(X_1), \dots, t(X_n), S_1, \dots, S_n, t(X)] \\ &\stackrel{(b)}{\geq} \frac{1}{2} P(\cap_{i=1}^n [k \neq k_i]) \\ &\stackrel{(c)}{=} \frac{1}{2} \sum_{k=1}^{\infty} p_k (1 - p_k)^n \end{aligned} \tag{28}$$

It remains to show that for all $\epsilon > 0$, we can choose $\{p_k\}$ such that the right hand side of inequality (28) is at least $1/2(1 - \epsilon)$. Let $\epsilon > 0$. We choose p_k as follows. First, pick $K > \frac{1}{1 - (1 - \epsilon)^{1/n}}$. Then, let $p_k = 1/K$ for $1 \leq k \leq K$ and $p_k = 0$ elsewhere. It follows that

$$\sup_{b \in [0,1]} E_{\mathcal{D}_n(b)} \text{BER}(f_n, t) \geq \frac{1}{2} \left(1 - \frac{1}{K}\right)^n \geq \frac{1}{2} (1 - \epsilon). \tag{29}$$

Therefore, using Lemma 6.1, we can conclude that for all $\epsilon > 0$, there exists a distribution over $\mathcal{X} \times \{0, 1\}$ such that for all auditors f_n

$$\Delta^*(t) - \Delta(f_n, t) \geq 1 - \epsilon. \tag{30}$$

6.4 Examples of Representation Mappings without Finite Sample Guarantees

Injective mappings. Suppose that t is injective from $[0, 1]^D$ to \mathbb{R}^d .

Consider X distributed over the countable and infinite set $\{1, 1/2, \dots, 1/k, \dots\}$ with $p_k = \kappa/k^2$ and $k^{-1} = \sum_{k=1}^{\infty} 1/k^2$. By lemma 6.2, $I_{\chi^2}(X, Z) = \infty$ and thus, by Corollary 2.2, there exists a distribution such that $\Delta^*(t) - \Delta(f_n, t) = 1$ for all f_n .

Large $t(\mathcal{X})$. Suppose that $|\{t(x)|x \in \mathcal{X}\}| \geq n/(\ln(n))^\alpha$, for some $\alpha < 1$.

By Lemma 6.2, $I_{\chi^2}(X, Z) \geq n/(\ln(n))^\alpha - 1$ and thus, by Corollary 2.1, if $\inf_{f_n \in \mathcal{F}_n} \sup_{\mu} E_{\mathcal{D}_n} |\Delta^*(t) - \Delta(f_n, t)| = \epsilon_n$, then

$$\begin{aligned} \frac{n}{(\ln(n))^\alpha} - 1 &\leq I_{\chi^2}(X, Z) \leq \frac{1}{1 - \epsilon_n^{\frac{1}{n}}} \\ &\stackrel{(a)}{\leq} \frac{n}{-\ln(\epsilon_n)}, \end{aligned} \tag{31}$$

where (a) uses that $e^{-x} \geq 1 - x$. Therefore, $\epsilon_n \geq e^{-(\ln(n))^\alpha} = \omega(n^{-s})$ for $s > 0$, since $\alpha < 1$.

6.5 Proof of Theorem 2.2

The proof Theorem 2.2 relies on an upper bound of $\Delta^*(t) - \Delta(f_n, t)$ that uses the total variation distance $TV(\mu_t^s, \mu_n^s)$ between class conditional densities and their empirical counterpart:

$$TV(\mu_t^s, \mu_n^s) = \int |\mu_t^s - \mu_n^s| dz. \tag{32}$$

Lemma 6.4. Consider a sample $\{(z_i, s_i)\}_{i=1}^n$ from a representation distribution μ_t induced by a representation rule t . Suppose that μ_n^0 and μ_n^1 are empirical density estimators of $P(Z|S=0)$ and $P(Z|S=1)$ respectively. Denote f_n the following auditing plug-in decision: for $z \in \mathcal{Z}$, $f_n(z) = 1$ if and only if $\mu_n^1(z) > \mu_n^0(z)$. Therefore, for all n

$$\Delta(f_n, t) \leq \Delta^*(t) \leq \Delta(f_n, t) + 2 \sum_{i=0,1} TV(\mu_t^i, \mu_n^i). \quad (33)$$

Proof. Let f^* denote the auditing rule that minimizes the balance error rate. Using [29] (ch 2), we show that for any auditing rule f_n

$$\begin{aligned} 2 - \int \eta_{f_n(z)}(z) \mu_t(dz) &= 2 - \sum_{i=0,1} \int_{f_n(z)=i} \eta_i(z) \mu_t(dz) \\ &= 2 - \sum_{i=0,1} \int_{f_n(z)=i} P(z|S=i) dz \\ &= 2BER(f_n), \end{aligned} \quad (34)$$

where $\eta_i(z)$ is the balanced posteriori probability $\eta_i(z) = P(S=i|Z=z)/P(S=i)$. Moreover,

$$\begin{aligned} 2BER(f^*) &= 2 - P(f^*(z) = 1|S=1] \\ &\quad - P(f^*(z) = 0|S=0) \\ &= 2 - \int_{z, \mu_t^1 > \mu_t^0} \mu_t^1(dz) - \int_{z, \mu_t^0 > \mu_t^1} \mu_t^0(dz) \\ &= 2 - \int \max_i \eta_i(z) \mu_t(dz). \end{aligned} \quad (35)$$

Let denote $\eta_{n,i}$ the empirical estimate of η_i . Using equations (34) and (35), the proof of lemma 6.4 relies on the fact that

$$\begin{aligned} BER(f_n) - BER(f^*) &= \int \max_i \eta_i(z) \mu_t(dz) \\ &\quad - \int \eta_{f_n(z)}(z) \mu_t(dz) \\ &= \int (\max_i \eta_i(z) - \max_i \eta_{n,i}(z)) \mu_t(dz) \\ &\quad + \int (\eta_{n,f_n(z)}(z) - \eta_{f_n(z)}(z)) \mu_t(dz) \\ &\stackrel{(a)}{\leq} \sum_{i=0,1} \int |\eta_i(z) - \eta_{n,i}(z)| \mu_t(dz) \\ &= \sum_{i=0,1} \int |\mu_t^i(z) - \mu_n^i(z)| dz, \end{aligned} \quad (36)$$

The inequality (a) comes from the following observation. If the maxima are attained for the same $i \in \{0, 1\}$, then the right hand side integrand is equal to 0. Otherwise, suppose without loss of generality that $\max \eta_i(z)$ is reached for $i = 0$, then the right hand side integrand is

$$\begin{aligned} \eta_0(z) - \eta_{n,1}(z) + \eta_{n,1}(z) - \eta_1(z) &= \eta_0(z) - \eta_{n,0}(z) \\ &\quad + \eta_{n,1}(z) - \eta_1(z) \\ &\quad + \eta_{n,0}(z) - \eta_{n,1}(z) \\ &\leq |\eta_0(z) - \eta_{n,0}(z)| \\ &\quad + |\eta_1(z) - \eta_{n,1}(z)|, \end{aligned} \quad (37)$$

where the inequality follows $\max_i \eta_{n,i}(z) = \eta_{n,1}(z)$. The same argument can be applied when $\max \eta_i(z) = \eta_1(z)$. The result in lemma 6.4 follows from (36). \square

The second part of the proof of theorem 2.2 is to show that the total variation distance between μ_n^s and μ_t^s is $O(1/\sqrt{n_s})$ for some empirical estimate of μ_t^s :

Lemma 6.5. *Consider a representation mapping $t : \mathcal{X} \rightarrow \mathcal{Z}$ and its induced distribution μ_t . Assume that $I_2(Z, X) < \infty$. Then, for $s = 0, 1$, define μ_n^s as*

$$\mu_n^s(z) = \frac{1}{n_s} \sum_{i=1, s_i=s}^n P(z|X = x_i) \quad (38)$$

The total variation between μ_t^s and μ_n^s can be bounded as follows:

$$E_{\mathcal{D} \sim \mathcal{X}^n} [TV(\mu_t^s, \mu_n^s)] \leq \sqrt{\frac{I_2(Z, X)}{n_s}}.$$

The upper bound of the total variation distance uses a Monte Carlo integration argument. For a sample $\mathcal{D}_n = \{x_i\}_{i=1}^n$, denote $\phi(z, x_i)$ the probability $P(Z = z|X = x_i)$. Therefore, $\mu_t(z) = E_{x \sim \mathcal{X}}[\phi(z, x)]$ and if μ_n^s is defined as in (38), $\mu_t^s(z) = E_{\mathbf{X}, S=s}[\mu_n^s]$, where $\mathbf{X} = \{x_i\}_{i=1}^n \sim \mathcal{X}^n$. Denote

$$\mathcal{E}^s(\mathbf{X}) = \int \left| \mu_t(z) - \frac{1}{n_s} \sum_{i=1, s_i=s}^n \phi(z, x_i) \right| dz, \quad (39)$$

with $n_s = |\{i|s_i = s\}|$. We have

$$\begin{aligned} E_{\mathbf{X}}[\mathcal{E}^s(\mathbf{X})] &\stackrel{(a)}{\leq} E_{\mathbf{X}} \left[\sqrt{\int \left(\frac{\mu_t(z) - \mu_n^s(z)}{\mu_t(z)} \right)^2 \mu_t(z) dz} \right] \\ &\stackrel{(b)}{=} \frac{1}{n_s} E_{\mathbf{X}} \left[\sqrt{\int \sum_{i=1, s_i=s}^n \left(\frac{\mu_t(z) - \phi(z, x_i)}{\mu_t(z)} \right)^2 \mu_t(z) dz} \right] \\ &\stackrel{(c)}{\leq} \frac{1}{n_s} \sqrt{E_{\mathbf{X}} \left[\int \sum_{i=1, s_i=s}^n \left(\frac{\mu_t(z) - \phi(z, x_i)}{\mu_t(z)} \right)^2 \mu_t(z) dz \right]} \\ &\stackrel{(d)}{=} \frac{1}{n_s} \sqrt{\sum_{i=1, s_i=s}^n E_{\mathbf{X}} \left[\int \left(\frac{\mu_t(z) - \phi(z, x_i)}{\mu_t(z)} \right)^2 \mu_t(z) dz \right]} \\ &\stackrel{(e)}{=} \sqrt{\frac{I_2(Z, X)}{n_s}}, \end{aligned} \quad (40)$$

where (a) applies Cauchy-Schwarz inequality; (b) uses the fact that the samples are independently drawn and that $E_{x_i}[\phi(z, x_i)] = \mu_t(z)$; (c) that the squared-root is concave; (d) that expectation and integral can be interchange; and, (e) the definition of the chi-squared mutual information between Z and X .

Putting lemma 6.4 and 6.5 together, we get the upper bound in theorem 2.2.

6.6 χ^2 versus Classic Mutual Information

Features are uniformly distributed over $[0, 1]$ and $t(x) = i$ for $x \in [1/(i+1), 1/i)$ and $i > 0$. For each $i > 0$, the sensitive attribute is constant over $[1/(i+1), 1/i)$ and equal to 1 with probability $1/2$.

From Lemma 6.2, it is clear that $I_{\chi^2}(X, Z) = \infty$. On the other hand, we can show that the classic mutual information between X and Z , $I_{Sh}(X, Z)$ is bounded. Since t is deterministic,

$$\begin{aligned}
I_{Sh}(X, Z) &= \sum_{i=1}^{\infty} \frac{\ln(i(i+1))}{i(i+1)} \\
&\leq \frac{\ln(2)}{2} + \int_1^{\infty} \frac{\ln(x(x+1))}{x^2} dx \\
&\stackrel{(a)}{=} \frac{\ln(2)}{2} + 1 + \int_1^{\infty} \frac{1}{x(x+1)} dx \\
&\stackrel{(b)}{\leq} \frac{\ln(2)}{2} + 2 < \infty,
\end{aligned} \tag{41}$$

where (a) and (b) use integration by part and (b) the fact that $1/x \geq 1/(x+1)$.

6.7 Proof if Theorem 3.1

We only prove the upper bound on the χ^2 mutual information since the remaining results in Theorem 3.1 follow directly from Theorem 2.2.

Since the mapping $(p, q) \rightarrow q(p/q - 1)^2$ is convex and since Z is an infinite mixtures of Gaussians, we have that for $x \in \mathcal{X}$

$$\begin{aligned}
&\int \left(\frac{\mu_{t^* \sigma}(z|X=x)}{\mu_{t^* \sigma}(z)} - 1 \right)^2 \mu_{t^* \sigma}(z) dz \\
\leq &\int \int \left(\frac{\mu_{t^* \sigma}(z|X=x)}{\mu_{t^* \sigma}(z|X=x')} - 1 \right)^2 \mu_{t^* \sigma}(z|X=x') dz \mu(dx') \\
&\stackrel{(a)}{=} \int \chi^2(z|X=x||z|X=x') \mu(dx'),
\end{aligned} \tag{42}$$

where we use Fubini Theorem to invert the summation over z and x' and (a) uses the definition of the χ^2 divergence between $p(z|X=x)$ and $p(z|X=x')$. Since both $p(z|X=x)$ and $p(z|X=x')$ are Gaussians with variance σ^2 and mean $t(x)$ and $t(x')$, respectively, the integrand in the right hand side of (42) can be computed analytically as

$$\begin{aligned}
&\chi^2(z|X=x||z|X=x') = \\
&\frac{1}{2} \left[\exp \left(\frac{\|t(x) - t(x')\|_2^2}{\sigma^2} \right) - 1 \right].
\end{aligned} \tag{43}$$

Therefore,

$$\begin{aligned}
I_{\chi^2}(X, Z) &\leq \frac{1}{2} E_{x, x'} \left[\exp \left(\frac{\|t(x) - t(x')\|_2^2}{\sigma^2} \right) \right] \\
&\leq \frac{1}{2} \exp \left(\frac{2\|t\|_{\infty}^2}{\sigma^2} \right).
\end{aligned} \tag{44}$$

6.8 Proof of Theorem 3.2

By [30], we know that the balanced error rate of the optimal auditor f^* is given by

$$\begin{aligned}
BER(f^*) &= \frac{1}{2} \int \min(\eta(z, 0), \eta(z, 1)) \mu_{t^* \sigma}(dz) \\
&= \frac{1}{4} \int (\eta(z, 0) + \eta(z, 1)) \mu_{t^* \sigma}(dz) \\
&\quad - \frac{1}{4} \int |\eta(z, 0) - \eta(z, 1)| \mu_{t^* \sigma}(dz) \\
&\stackrel{(a)}{=} \frac{1}{2} - \frac{1}{4} \int |\eta(z, 0) - \eta(z, 1)| \mu_{t^* \sigma}(dz),
\end{aligned} \tag{45}$$

where (a) uses the definition of $\eta(z, s) = P(Z = z|S = s)/P(z)$. Therefore, by Lemma 6.1,

$$\mathcal{L}_{DP}(\mu_{t,\sigma}) = \frac{1}{2} \int |\mu_{t,\sigma}^0(z) - \mu_{t,\sigma}^1(z)| dz \quad (46)$$

and that

$$\mathcal{L}_{DP}(\mu_{n,\sigma}) = \frac{1}{2} \int |\mu_{n,\sigma}^0(z) - \mu_{n,\sigma}^1(z)| dz. \quad (47)$$

Therefore, for any t and any features distribution μ over the features \mathcal{X} ,

$$\begin{aligned} |\mathcal{L}_{DP}(\mu_{n,\sigma}) - \mathcal{L}_{DP}(\mu_{t,\sigma})| &\stackrel{(a)}{\leq} \int |(\mu_{t,\sigma}^0(z) - \mu_{t,\sigma}^1(z)) \\ &\quad - (\mu_{n,\sigma}^0(z) - \mu_{n,\sigma}^1(z))| dz \\ &\stackrel{(b)}{\leq} \int |(\mu_{t,\sigma}^0(z) - \mu_{n,\sigma}^0(z))| dz \\ &\quad + \int |(\mu_{t,\sigma}^1(z) - \mu_{n,\sigma}^1(z))| dz \\ &\stackrel{(c)}{\leq} \exp\left(\frac{\|t\|_\infty^2}{\sigma^2}\right) \left(\sqrt{\frac{1}{n_0}} + \sqrt{\frac{1}{n_1}}\right), \end{aligned} \quad (48)$$

where (a) and (b) are consequences of triangular inequalities; and (c) follows from the definition of total variation distance, the upper bound in lemma 6.5 and theorem 3.1.

6.9 Monte Carlo Approximation

Lemma 6.6. *let $m > 0$ and $n > 0$. Consider a sample $\{(x_i, s_i)\}$ and a noise vector $\{noise_{ji}\}$ of $n \times m$ draws from a d -dimensional Gaussian $\mathcal{N}(0, \sigma I_d)$. Denote $\mu_{n,\sigma}$ the empirical density as in (38) and for $i = 1, \dots, n$ and $j = 1, \dots, m$ $z_{ij} = t(x_i) + noise_{ij}$. If*

$$\hat{\mathcal{L}}_{DP}(\mu_{n,\sigma}) = \frac{1}{nm} \sum_{i=1}^n \sum_{j=1}^m |\eta_n(z_{ij}, 1) - \eta_n(z_{ij}, 0)| \quad (49)$$

then $\hat{\mathcal{L}}_{DP}(\mu_{n,\sigma})$ is an unbiased estimator of $\mathcal{L}_{DP}(\mu_{n,\sigma})$ and

$$E_{noise} \left[(\hat{\mathcal{L}}_{DP}(\mu_{n,\sigma}) - \mathcal{L}_{DP}(\mu_{n,\sigma}))^2 \right] \leq \frac{8\|t\|_\infty^2 + 4\sigma^2}{\sigma^2} \frac{1}{nm}. \quad (50)$$

Proof. First, $\hat{\mathcal{L}}_{DP}(\mu_{n,\sigma})$ is an unbiased estimator of $\mathcal{L}_{DP}(\mu_{n,\sigma})$ because

$$\begin{aligned} E_{noise} \left[\hat{\mathcal{L}}_{DP} \right] &= \frac{1}{nm} \sum_{i=1}^n \sum_{j=1}^m E_{noise} [|\eta_n(z_{ij}, 1) - \eta_n(z_{ij}, 0)|] \\ &= \frac{1}{nm} \sum_{i=1}^n \sum_{j=1}^m \mathcal{L}_{DP}(\mu_{n,\sigma}) \\ &= \mathcal{L}_{DP}(\mu_{n,\sigma}). \end{aligned} \quad (51)$$

Therefore, the mean squared error can be written as

$$\begin{aligned} E_{noise} \left[(\hat{\mathcal{L}}_{DP}(\mu_{n,\sigma}) - \mathcal{L}_{DP}(\mu_{n,\sigma}))^2 \right] \\ = \frac{1}{n^2 m} \sum_{i=1}^n var_{noise} [k(x_i + noise)], \end{aligned} \quad (52)$$

where $k(z) = |\eta_n(z, 1) - \eta_n(z, 0)|$. Moreover, by Gaussian Poincare inequality,

$$\begin{aligned} var_{noise} [k(x_i + noise)] &\stackrel{(a)}{\leq} \sigma^2 E_{noise} \|\nabla k(x_i + noise)\|_2^2 \\ &\stackrel{(b)}{=} 2\sigma^2 \sum_s E_{noise} \left[\|\nabla \log(\mu_{n,\sigma}^s(z, s))\|_2^2 \right] \end{aligned} \quad (53)$$

where (a) uses the fact that the noise is Gaussian with standard deviation σ ; (b) that $z = x_i + \text{noise}$ and that $\nabla \eta_n(z, s) = \eta_n(z, s) \nabla \log(\mu_{n,\sigma}^s(z, s)) + (1 - \eta_n(z, s)) \nabla \log(\mu_{n,\sigma}^s(z, 1 - s))$. Moreover, for $s = 0, 1$

$$\begin{aligned} \nabla \log(\mu_{n,\sigma}^s(z, s)) &\stackrel{(a)}{=} \sum_{i=1}^n \nabla \log(\phi(z, x_i)) P(X = x_i | z) \\ &= -\frac{1}{2\sigma^2} \sum_{i=1}^n (z - t(x_i)) P(X = x_i | z), \end{aligned} \quad (54)$$

where (a) denotes the Gaussian density with mean $t(x)$ and standard deviation σ as $\phi(z, x)$. Therefore,

$$\|\nabla \log(\mu_{n,\sigma}^s(z, s))\|_2 \leq \frac{\|z\|_2 + \|t\|_\infty}{\sigma^2}. \quad (55)$$

□

Moreover, $z \sim \mu_{n,\sigma}$, which is a mixture of n Gaussians, each with a non-central second moment equal to $\sigma^2 + \|t(x_i)\|^2$. Therefore,

$$E_{\text{noise}} \|z\|_2^2 \leq \sigma^2 + \|t\|_\infty^2. \quad (56)$$

By combining (53), (54) (55) and (56), we obtain that

$$\text{var}_{\text{noise}} [k(x_i + \text{noise})] \leq 4 \frac{2\|t\|_\infty^2 + \sigma^2}{\sigma^2}, \quad (57)$$

and thus that

$$E_{\text{noise}} \left[(\hat{\mathcal{L}}_{DP}(\mu_{n,\sigma}) - \mathcal{L}_{DP}(\mu_{n,\sigma}))^2 \right] \leq 4 \frac{2\|t\|_\infty^2 + \sigma^2}{\sigma^2 nm} \quad (58)$$

References

- [1] ProPublica. How we analyzed the compas recidivism algorithm. *ProPublica*, 2016.
- [2] Joy Buolamwini and Timnit Gebru. Gender shades: Intersectional accuracy disparities in commercial gender classification. In Sorelle A. Friedler and Christo Wilson, editors, *Proceedings of the 1st Conference on Fairness, Accountability and Transparency*, volume 81 of *Proceedings of Machine Learning Research*, pages 77–91, New York, NY, USA, 23–24 Feb 2018. PMLR.
- [3] Josh Gardner, Christopher Brooks, and Ryan Baker. Evaluating the fairness of predictive student models through slicing analysis. In *Proceedings of the 9th International Conference on Learning Analytics & Knowledge*, pages 225–234. ACM, 2019.
- [4] Stephen Pfohl, Ben Marafino, Adrien Coulet, Fatima Rodriguez, Latha Palaniappan, and Nigam H Shah. Creating fair models of atherosclerotic cardiovascular disease risk. In *Proceedings of the 2019 AAAI/ACM Conference on AI, Ethics, and Society*, pages 271–278. ACM, 2019.
- [5] David Madras, Elliot Creager, Toniann Pitassi, and Richard Zemel. Learning adversarially fair and transferable representations, 2018.
- [6] Elliot Creager, David Madras, Jörn-Henrik Jacobsen, Marissa A. Weis, Kevin Swersky, Toniann Pitassi, and Richard S. Zemel. Flexibly fair representation learning by disentanglement. *ArXiv*, abs/1906.02589, 2019.
- [7] Harrison Edwards and Amos Storkey. Censoring representations with an adversary. *arXiv preprint arXiv:1511.05897*, 2015.
- [8] Rich Zemel, Yu Wu, Kevin Swersky, Toni Pitassi, and Cynthia Dwork. Learning fair representations. In *International Conference on Machine Learning*, pages 325–333, 2013.
- [9] Alexandra Chouldechova and Aaron Roth. The frontiers of fairness in machine learning. *arXiv preprint arXiv:1810.08810*, 2018.
- [10] Ziv Goldfeld, Kristjan Greenewald, Yury Polyanskiy, and Jonathan Weed. Convergence of smoothed empirical measures with applications to entropy estimation. *arXiv preprint arXiv:1905.13576*, 2019.
- [11] Cynthia Dwork, Moritz Hardt, Toniann Pitassi, Omer Reingold, and Richard Zemel. Fairness through awareness. In *Proceedings of the 3rd innovations in theoretical computer science conference*, pages 214–226, 2012.

- [12] Alekh Agarwal, Alina Beygelzimer, Miroslav Dudík, John Langford, and Hanna Wallach. A reductions approach to fair classification. *arXiv preprint arXiv:1803.02453*, 2018.
- [13] Michael Kim, Omer Reingold, and Guy Rothblum. Fairness through computationally-bounded awareness. In *Advances in Neural Information Processing Systems*, pages 4842–4852, 2018.
- [14] Michael Kearns, Seth Neel, Aaron Roth, and Zhiwei Steven Wu. Preventing fairness gerrymandering: Auditing and learning for subgroup fairness. In *International Conference on Machine Learning*, pages 2569–2577, 2018.
- [15] Michael Feldman, Sorelle A Friedler, John Moeller, Carlos Scheidegger, and Suresh Venkatasubramanian. Certifying and removing disparate impact. In *Proceedings of the 21th ACM SIGKDD International Conference on Knowledge Discovery and Data Mining*, pages 259–268. ACM, 2015.
- [16] Xavier Gitiaux and Huzefa Rangwala. mdfa: Multi-differential fairness auditor for black box classifiers. In *IJCAI*, 2019.
- [17] Jon Kleinberg, Sendhil Mullainathan, and Manish Raghavan. Inherent trade-offs in the fair determination of risk scores. *arXiv preprint arXiv:1609.05807*, 2016.
- [18] Moritz Hardt, Eric Price, and Nathan Srebro. Equality of opportunity in supervised learning, 2016.
- [19] Toon Calders and Indrè Žliobaitė. Why unbiased computational processes can lead to discriminative decision procedures. In *Discrimination and privacy in the information society*, pages 43–57. Springer, 2013.
- [20] Paula Gordaliza, Eustasio Del Barrio, Gamboa Fabrice, and Jean-Michel Loubes. Obtaining fairness using optimal transport theory. In *International Conference on Machine Learning*, pages 2357–2365, 2019.
- [21] Flavio Calmon, Dennis Wei, Bhanukiran Vinzamuri, Karthikeyan Natesan Ramamurthy, and Kush R Varshney. Optimized pre-processing for discrimination prevention. In I. Guyon, U. V. Luxburg, S. Bengio, H. Wallach, R. Fergus, S. Vishwanathan, and R. Garnett, editors, *Advances in Neural Information Processing Systems 30*, pages 3992–4001. Curran Associates, Inc., 2017.
- [22] Karol Kurach, Mario Lucic, Xiaohua Zhai, Marcin Michalski, and Sylvain Gelly. A large-scale study on regularization and normalization in gans, 2018.
- [23] Yaroslav Ganin, Evgeniya Ustinova, Hana Ajakan, Pascal Germain, Hugo Larochelle, François Laviolette, Mario Marchand, and Victor Lempitsky. Domain-adversarial training of neural networks. *The Journal of Machine Learning Research*, 17(1):2096–2030, 2016.
- [24] Brian Hu Zhang, Blake Lemoine, and Margaret Mitchell. Mitigating unwanted biases with adversarial learning. In *Proceedings of the 2018 AAAI/ACM Conference on AI, Ethics, and Society*, pages 335–340, 2018.
- [25] Depeng Xu, Shuhan Yuan, Lu Zhang, and Xintao Wu. Fairgan: Fairness-aware generative adversarial networks. In *2018 IEEE International Conference on Big Data (Big Data)*, pages 570–575. IEEE, 2018.
- [26] Christos Louizos, Kevin Swersky, Yujia Li, Max Welling, and Richard Zemel. The variational fair autoencoder, 2015.
- [27] Luca Oneto, Michele Donini, Andreas Maurer, and Massimiliano Pontil. Learning fair and transferable representations, 2019.
- [28] Cynthia Dwork, Aaron Roth, et al. The algorithmic foundations of differential privacy. *Foundations and Trends® in Theoretical Computer Science*, 9(3–4):211–407, 2014.
- [29] Luc Devroye, László Györfi, and Gábor Lugosi. *A probabilistic theory of pattern recognition*, volume 31. Springer Science & Business Media, 2013.
- [30] Ming-Jie Zhao, Narayanan Edakunni, Adam Pocock, and Gavin Brown. Beyond fano’s inequality: bounds on the optimal f-score, ber, and cost-sensitive risk and their implications. *Journal of Machine Learning Research*, 14(Apr):1033–1090, 2013.
- [31] Loic Matthey, Irina Higgins, Demis Hassabis, and Alexander Lerchner. dsprites: Disentanglement testing sprites dataset. <https://github.com/deepmind/dsprites-dataset/>, 2017.
- [32] Thomas M Cover and Joy A Thomas. *Elements of information theory*. John Wiley & Sons, 2012.